JOURNAL OF MATERIALS SCIENCE 26 (1991) 4829–4835

Elaboration and characterization of $YBa_2Cu_3O_{7-x}$ thick tapes

C. HIS, N. CHARDON, R. KUENTZLER, S. VILMINOT
Groupe des Matériaux Inorganiques, IPCMS EHICS, 1 rue Blaise Pascal, 67008 Strasbourg, France

Thick tapes of $YBa_2Cu_3O_{7-x}$ superconductor have been tape-cast by the Doctor Blade technique. Sintering at temperatures higher than 950 °C reveals a texturing with (001) planes preferentially aligned parallel to the tape surface. The transition temperature and width as well as the resistivity at onset temperature are related to the sintering parameters. Low-temperature specific heat measurements show the disappearance of the upturn at low temperature, usually observed for this material.

1. Introduction

Since the discovery by Bednorz and Müller [1] of superconductivity in copper based oxides, a lot of work has been performed on these materials in a search for compounds with still higher T_c. It has yielded an increase of T_c above liquid nitrogen with $YBa_2Cu_3O_{7-x}$ [2], Bi and Tl based systems [3, 4]. As far as $YBa_2Cu_3O_{7-x}$ is concerned, it appears that, if T_c is always reproducible, other properties are strongly dependent on sample processing: ceramics, thin films, single crystals, etc. For critical currents, differences of three to four orders of magnitude are observed, with values around 10^3 A cm^{-2} and 10^6–10^7 A cm^{-2} for ceramics [5] and thin films or single crystals [6, 7], respectively. Many factors can contribute to the observed differences. First of all, measurements on single crystals put into evidence the anisotropy of the resistive properties. From a chemical point of view, oxygen stoichiometry, as x in the formulae $YBa_2Cu_3O_{7-x}$, can be dependent on sample processing. Bulk materials such as ceramics do not behave in the same manner towards the reoxidation process which takes place at moderate temperature (around 450 °C) as do thin films with a larger reaction area. Another factor that has been considered concerns the microstructure of the samples. Measurements of transport critical current density, J_c [8], indicate that the transport J_c is dominated, for bulk ceramics, by weak-link regions between high T_c regions.

This paper deals with the elaboration of tape-cast $YBa_2Cu_3O_{7-x}$ thick films with thickness of around 100 μm. Such a process involves the control of different steps like powder elaboration, powder granulometry, slurry elaboration and, finally, sintering. The resulting samples have been characterized by X-ray diffraction, resistivity and low-temperature specific heat measurements.

2. Experimental procedure

2.1. Powder elaboration and characterization

The first step concerns the elaboration of the superconducting $YBa_2Cu_3O_{7-x}$ powder. Realization of tapes with limited thickness involves the control of the granulometry of the starting powder. According to our experiments, solid state reaction between the constituent oxides and/or carbonates yields a strong increase of the grain mean size due to the high temperature (940–950 °C) of calcination. It is necessary to grind the powder before use. An alternative process is to lower the reaction temperature in order to avoid grain growth. Chemical methods such as oxalate coprecipitation [9], metallo-organic decomposition [10] and citrate route [11], allow the reaction temperature to be decreased and fine powders to be obtained.

We have used the oxalate route for the precursor elaboration. This precursor is currently synthesized by Criceram in batches of a few kilograms.

Previous studies [12] have shown that calcination under air flow of the oxalate mixture yields first, after oxalate group decomposition, yttrium and copper oxides and barium carbonate. The ternary phase formation starts around 800 °C and is achieved at 850 °C.

X-ray diffraction measurements show that the orthorhombicity $(a–b)/b$, is dependent on the reaction temperature (Table I). We therefore chose 900 °C as the reaction temperature. At this temperature, granulometric measurements and SEM observations reveal that grain growth is still limited.

TABLE I Evolution of the orthorhombicity, $(b–a)/b$, with calcination temperature

T(°C)	$(b–a)/b$
800	0^a
825	0.007
850	0.0138
875	0.0160
900	0.0163
925	0.0173
950	0.0180

[a] At this temperature, $YBa_2Cu_3O_{7-x}$ appears to be tetragonal and a small amount of residual $BaCO_3$ is detected by X-ray diffraction.

In order to check the influence of grinding, the oxalate precursor, issued from the same batch, had also been reacted at 940 °C. A slight increase of the orthorhombicity (Table I) is observed.

Both powders (900 and 940 °C) have been characterized by granulometric measurements, SEM observation and X-ray diffraction.

Granulometric measurements have been performed using a Malvern 3600 E apparatus, using the principle of diffraction of a laser beam from particles dispersed in a liquid (absolute ethanol in our case). One observes an increase in agglomerate size with increasing temperature and a broadening of the dispersity (Fig. 1). Scanning electron microscope (SEM) observations confirm these results and allow determination of the mean grain size instead of the agglomerate size (Fig. 2). The micrographs reveal a difference in morphology between both kinds of samples (900 and 940 °C). Whereas, for the higher temperature, the particles exhibit plate-like morphology, for the lowest temperature, they appear to be more isotropic. The grain sizes are also different with an homogeneous distribution of around 2–3 μm for 900 °C calcination and a highly polydispersed distribution for 950 °C calcination ranging from 1–50 μm.

As the slurry elaboration needs around 50 g powder, the oxalate precursor has been calcinated in batches of 300 g. Even using large containers, the powder thickness is quite important and we systematically observe the formation of a small quantity of the green phase, Y_2BaCuO_5 at the surface of the sample in contact with the container. If the green phase is present, from stoichiometric considerations, other impurity phases are also formed, i.e. $BaCuO_{2+x}$ and

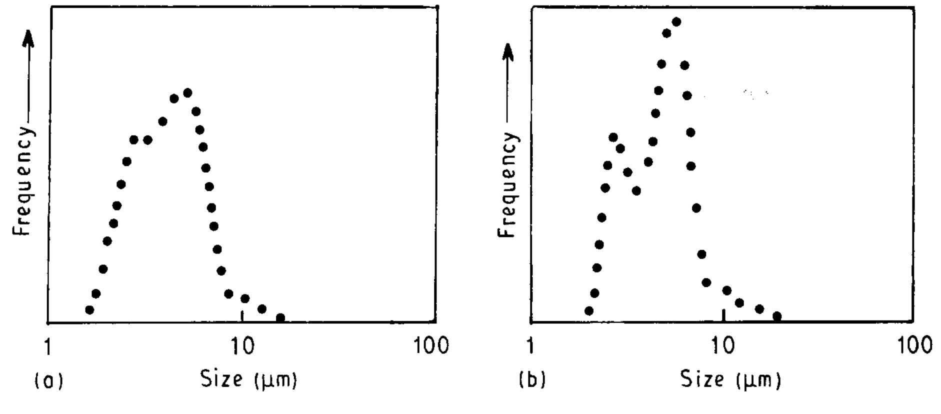

Figure 1 Evolution of the agglomerate sizes with calcination temperature: (a) 800 °C, (b) 850 °C (c) 900 °C, (d) 940 °C.

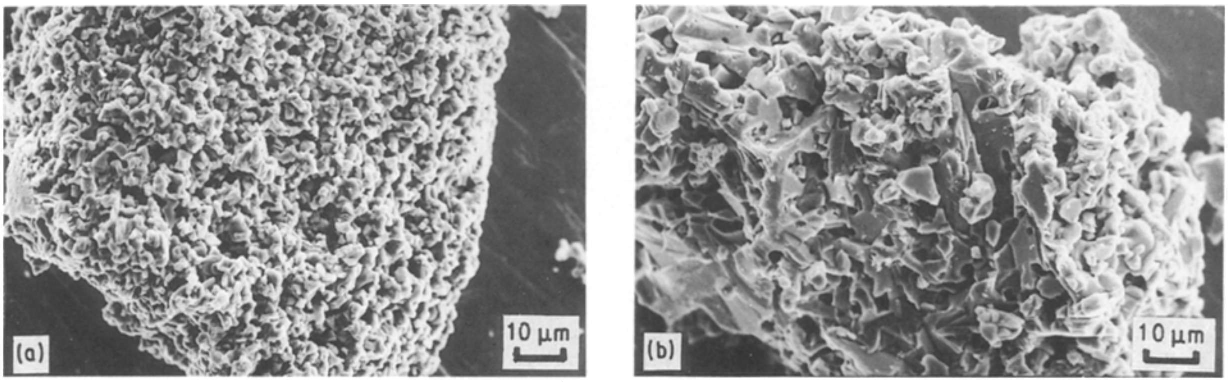

Figure 2 Scanning electron micrographs of $YBa_2Cu_3O_{7-x}$ powders obtained after (a) 900 °C, and (b) 940 °C calcinations.

CuO X-ray diffraction measurements revealed the presence of two extra-lines, corresponding to d-spacings around 0.3 nm. These can be attributed to Y_2BaCuO_5 and $BaCuO_{2+x}$, whereas CuO does not appear.

In order to avoid the presence of too big particles in the slurry, grinding was performed on the powder calcined at 940 °C.

2.2. Granulometry control

As previously mentioned, the powder obtained after calcination at 900 °C appears to be suitable for slurry elaboration without grinding.

For the 940 °C powder, we have followed the agglomerate size evolution according to the grinding time. Grinding has been performed by ball-milling using an agathe mortar, the powder being dispersed in absolute ethanol. Fig. 5 shows the evolution of agglomerate size distribution with time. It appears that the narrower dispersity is achieved after 24 h. Further grinding (48 h duration) yields a broadening of the agglomerate size distribution, even if smaller particles can be obtained. We have therefore considered that 24 h duration grinding is better in view of the slurry elaboration.

Both 900 and 940 °C calcinations have been qualitatively checked for their diamagnetic properties at the temperature of liquid nitrogen. This simple test, repulsion of a pellet placed near a permanent magnet, reveals that both powders are diamagnetic. However, it has been noticed that after grinding no more Meissner effect is detected. Magnetic susceptibility measurements confirm this observation (Fig. 3). We have measured the evolution with temperature of the magnetic susceptibility for powders with different grinding times. The sample is first cooled down to the lowest temperature at which it is without magnetic field (ZFC = zero field cooling). The susceptibility is then measured with increasing temperature under an external field of 8×10^{-2} Tesla. One observes a strong decrease in the absolute value of magnetic susceptibility with increasing grinding time. This behaviour is related to the decrease in particle size, which can become lower than the penetration length, λ, which is the distance along which the applied field enters the sample. For $YBa_2Cu_3O_{7-x}$, λ is around 0.1–0.2 μm. Further calcination allows grain growth and the Meissner effect to be restored.

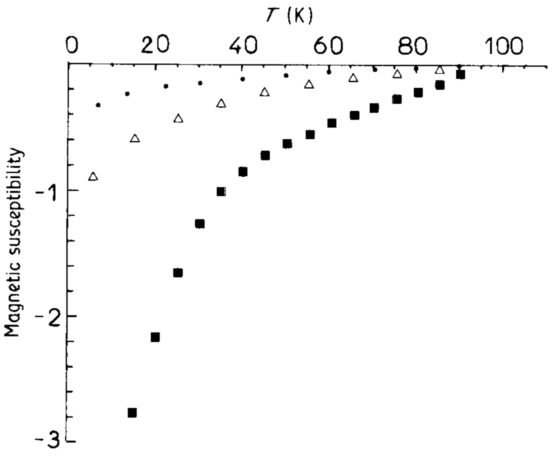

Figure 3 ZFC magnetic susceptibility measurements on powders with different griding times: (■) 0 h, (△) 15 h, (●) 48 h.

2.3. Tape-cast slurry elaboration

The next step concerns the slurry elaboration from both kinds of powders. The main constituents of the slurry are, besides the powder, the solvent, the dispersant, the binder and the plasticizer. The slurry formulation means to find the relative proportions of each constituent in order to get an homogeneous mixture where the powder is perfectly dispersed. The viscosity and composition have to be adjusted in order to allow the tape to be stripped off the substrate and to exhibit good mechanical properties.

Different solvents have been checked and need the following requirements: no reactivity with the powder; the ability to dissolve the dispersant, binder and plasticizer; the ability to disperse the powder; a low evaporation temperature and no toxicity.

From sedimentation experiments, it appears that MEK/ethanol azeotrope (66/34 wt %) can be used as the solvent (MEK = methylethylketone). The $YBa_2Cu_3O_{7-x}$ powder is mixed with appropriate amounts of solvent, dispersant, binder and plasticizer for 4 h in ZrO_2 media to obtain an homogeneous slip. Thick tapes (75–200 μm) are cast on polypropylene film by the Doctor Blade technique. The tapes are dried in air and stripped off the polypropylene film. The green tapes are highly flexible and rubber-like.

2.4. Sintering

The tapes are subsequently sintered at different temperatures for different time periods in a tube furnace under an oxygen atmosphere. In order to avoid a possible deformation of the tape during the burning and decomposition of the organic constituents, we first proceed to a 2 h duration calcination around 400 °C, this temperature being reached at a $50\,°C\,h^{-1}$ rate. The temperature is then increased to the sintering one at a $150\,°C\,h^{-1}$ rate. The decrease rate has been chosen as $100\,°C\,h^{-1}$ for all samples. Some results concerning the sinterability of the samples are shown in Table II.

TABLE II Sinterability of both kinds of tapes

Calcination temperature (°C)	Temperature (°C)	Sintering shrinkage	
		(%)	d/d_{th}
940	950	18	0.8
+ grinding	960	23	0.9
	970	24	0.95
	980	25	[a]
900	930	6	0.6
	960	16	0.92
	970	18	0.95
	980	18	0.96

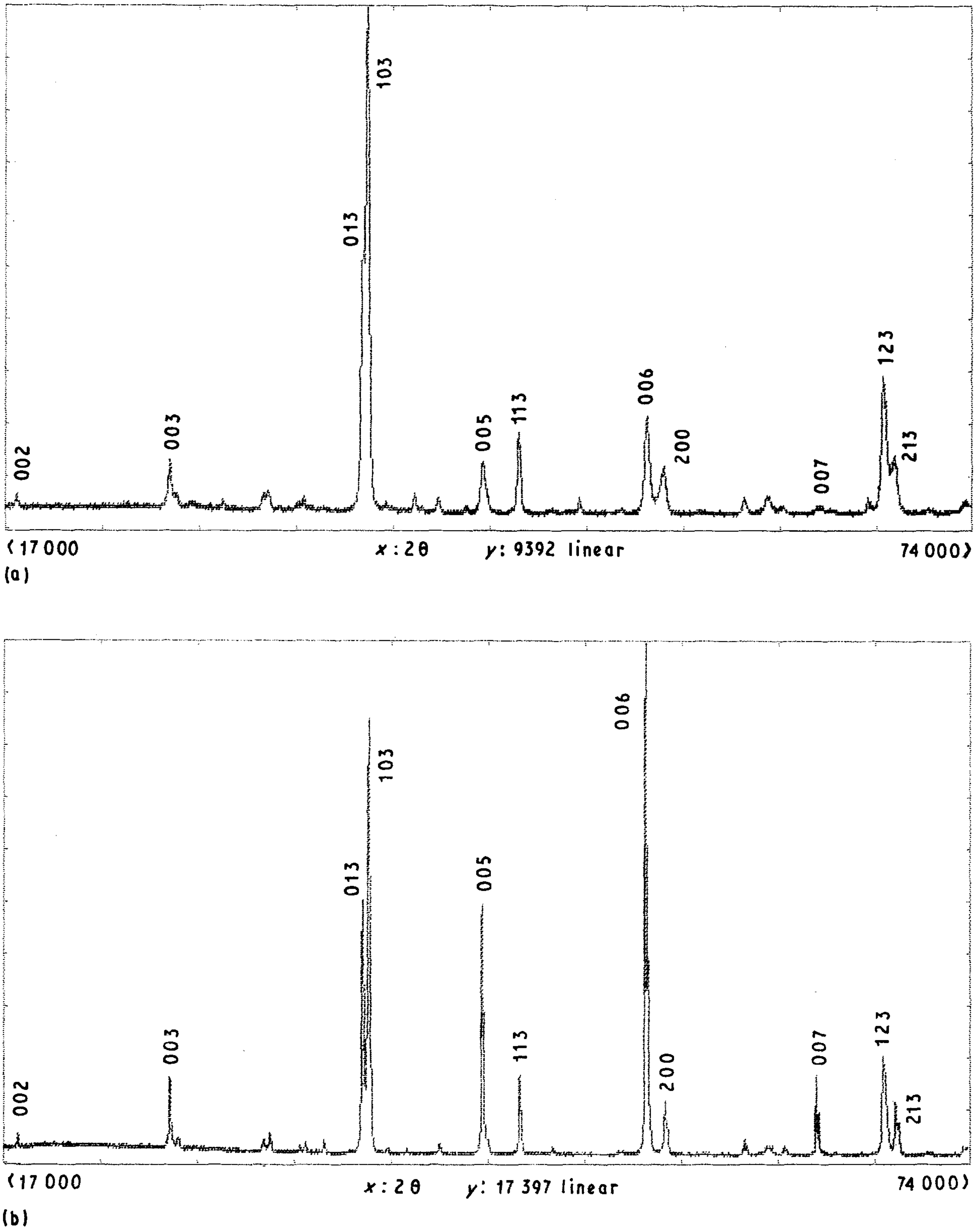

Figure 4 X-ray diffraction patterns of (a) powder and (b) tape.

From these results, a few remarks can be made. Sintering is only achieved at temperatures higher than 960 °C. Starting from the same powders, it has been observed that bulk ceramics can be decomposed or melted in this temperature domain under the same conditions. This behaviour could be related to the thickness of the samples: for the tapes, oxygen exchange with the surrounding atmosphere is much more effective and serves to stabilize the ternary compound. A smaller shrinkage for the tapes made from the 900 °C calcination powder yields the same final densities or even higher values. This can be related to a better green density. Finally, the sintering temperature is related to the tape thickness: the higher the thickness, the lower the sintering temperature.

3. Sample characterizations

3.1. X-ray diffraction

The X-ray studies have been performed on the sintered tapes by means of CoK_α radiation on a Siemens D 500 diffractometer. Fig. 4 shows the corresponding

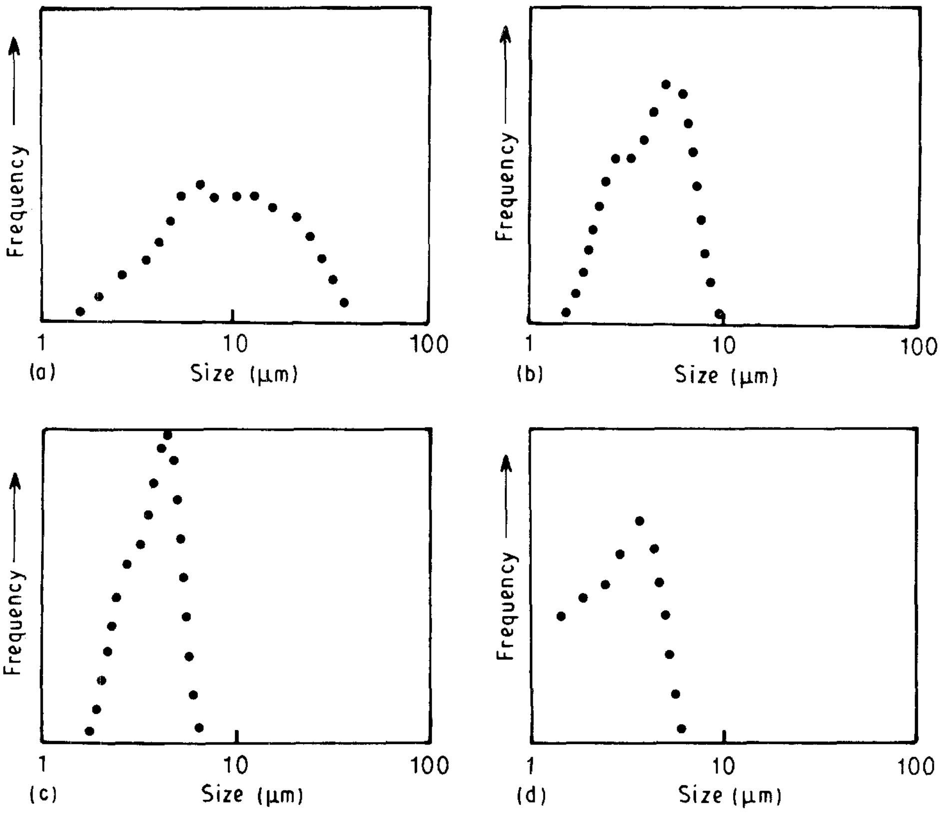

Figure 5 Influence of grinding time on the size distributions: (a) 0 h, (b) 15 h, (c) 24 h, (d) 48 h.

diffraction patterns for the tapes and for the powder that was used in the fabrication of the slurry. It is clear that the relative intensities of the (0 0 l) peaks are much higher for the tapes than for the randomly oriented powders. Whereas (h k l) peaks have their relative intensities equal or even lower, the (0 0 l) peaks are enhanced by a factor of 4. This indicates that, during sintering, a strongly anisotropic grain growth takes place, the crystals being preferentially aligned with their (0 0 l) planes parallel to the tape surface. The observed preferred orientation of the crystallites in the tape is expected to improve the critical current density, J_c [6, 7, 13]. Using the same process, Singh *et al.* [14] have also observed preferred orientations.

3.2. Resistivity measurements

The d.c. resistivity measurements have been made using a conventional four-probe technique on 30 mm × 4 mm × 0.12 mm size samples with a current of 10 mA. All samples sintered above 950 °C are superconducting at the temperature of liquid nitrogen. The sintering temperature and time have an influence on the resistivity results (ΔT_c, zero resistivity temperature, T_0 and resistivity at onset temperature, ρ_{on}): better characteristics are obtained for a higher temperature with shorter time (Table III). As shown in Fig. 6, a sharp transition is observed and a good metallic behaviour appears above T_c. Unfortunately, J_c measurements performed at 77 K do not reveal any enhancement compared to bulk ceramics with values around 120 A cm^{-2}.

TABLE III Resistivity measurements

Sintering temperature (°C)	Time (h)	T_0(K)	ρ_{on} (μΩ cm)	ΔT_c(K)
950	8	94	465	3.3
960	8	92.9	320	1.2
970	8	92	340	1.9
984	8	91	380	3.2
990	8	90	640	3.2
990	1	92.8	190	1.2
982	60	87.2	5000	6.5

3.3. Low-temperature specific heat measurements

All reports [15] on the low temperature specific heat of the $YBa_2Cu_3O_{7-x}$ high T_c oxide have mentioned a non-zero linear term and an upturn in the low temperature C/T in addition to a T^3 lattice term. This is surprising, as in a superconductor at $T \ll T_c$, one expects the specific heat to be the sum of an exponential electronic term and of a Debye cubic lattice term. No completely satisfying explanation has yet evolved for this anomalous behaviour. The upturn in C/T is generally thought to originate from the presence of a small amount of parasitic phases and we have proposed [16] that $BaCuO_{2+x}$ could have the strongest influence. The linear term of the specific heat, γ^*, appears to be sample dependent but no correlation has yet been established between γ^* and the superconducting transition temperature, T_c, or any other physical property. It is interesting to compare the specific heat evolutions for tapes and bulk ceramics. Fig. 7 shows the specific heat evolution plotted as C/T versus T^2 for both kinds of samples in

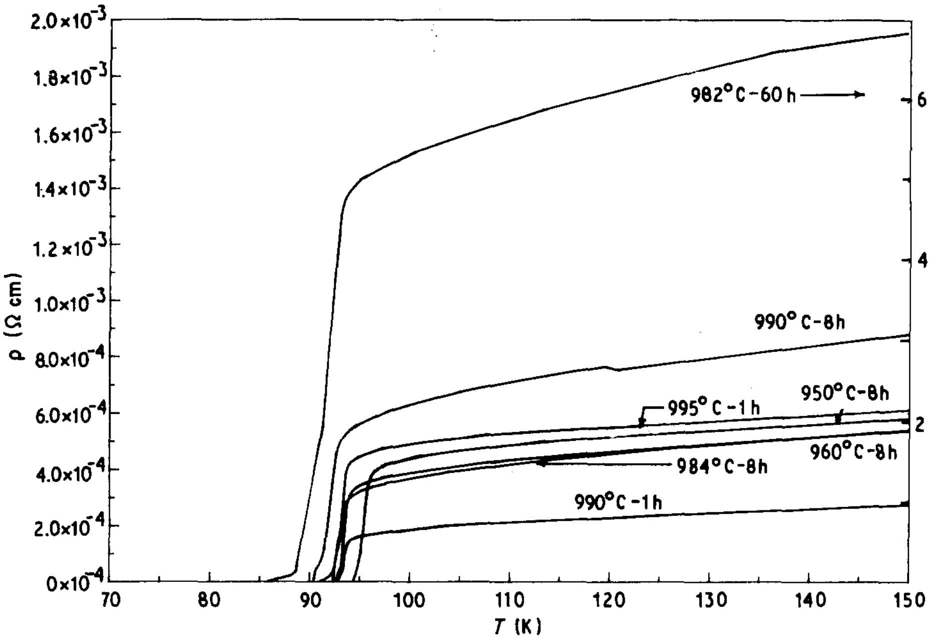

Figure 6 Resistivity evolution versus temperature for samples sintered at different temperatures.

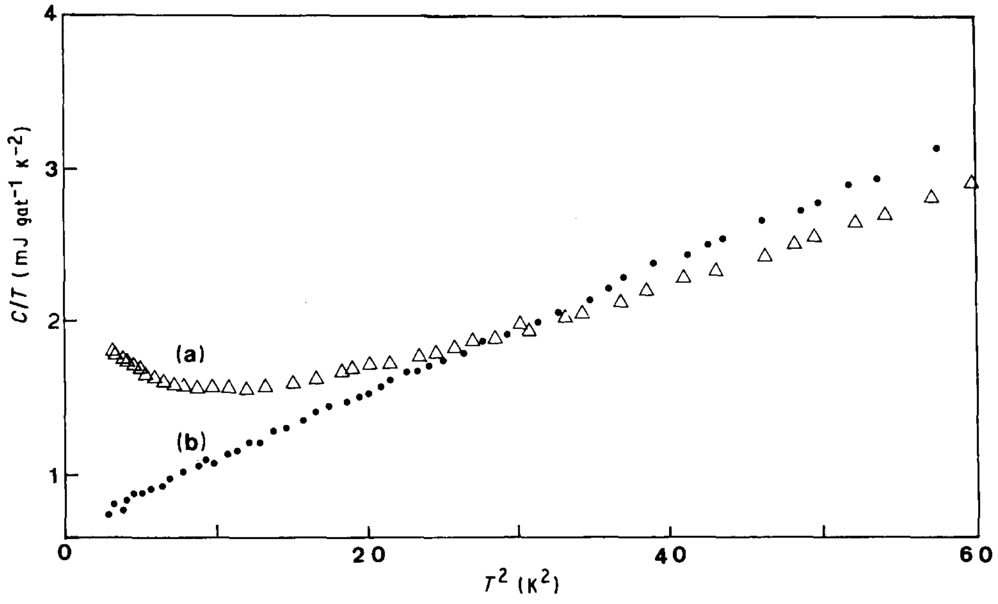

Figure 7 Low temperature specific heat evolution for (a) bulk ceramics and (b) tape.

the temperature range 1.5–8 K. In both cases, the specific heat at low temperature exhibits a linear evolution as $C = \gamma T + \beta T^3$, with $\gamma = 0.95$ mJ gat^{-1} K^{-2} and $\gamma = 0.60$ mJ gat^{-1} K^{-2} for bulk ceramics and tape, respectively. These results seem to indicate that tape processing improves the sample quality. It appears that the upturn at low temperature has completely disappeared in the case of the tape.

4. Conclusions

Tape casting appears to be an interesting way of obtaining thick films with preferred orientations in the case of $YBa_2Cu_3O_{7-x}$. Low-temperature specific heat measurements seem to indicate an improvement of the chemical homogeneity with the absence of an upturn at low temperature. However, much work has still to be done in order for higher J_c values to be obtained.

References

1. J. G. BEDNORZ and K. A. MÜLLER, *Z. Physik* **B64** (1986) 189.
2. C. W. CHU, P. H. HOR, R. L. MENG, L. GOA, Z. J. HUANG and Y. Z. WANG, *Phys. Rev. Lett.* **58** (1987) 405.
3. H. MAEDA, Y. TANAKA, M. FUKUTOMI and T. ASANO, *Jpn J. Appl. Phys.* **27** (1988) L209.
4. Z. Z. SHENG, A. M. HERMAN, A. EL ALI, C. ALMASAN, J. ESTRADA and T. DATTA, *Phys. Rev. Lett.* **60** (1988) 1937.
5. R. J. CAVA, B. BATLOGG, R. B. van DOVER, D. W. HURPHY, S. SUNSHINE, T. SIEGRIST, J. P. REMEIKA, E. A. RIETMAN, S. ZAHURAK and G. ESPINOZA, *ibid.* **58** (1987) 1676.
6. P. CHAUDHARY, R. H. KOCH, R. B. LAIBOWITZ, T. R. Mc GUIRE and R. J. CAMBINO, *ibid.* **58** (1987) 2684.
7. T. R. DINGER, T. K. WORTHINGTON, W. J. GALLAGHER and R. L. SANDSTORM, *ibid.* **58** (1987) 2687.
8. J. W. EKIN, A. I. BRAGINSKI, A. J. PANSON, M. A. JANOCKO, D. W. CAPONE, N. ZALUZEC, B. FLANDERMEYER, O. F. de LIMA, H. HONG, J. KWO and S. H. LIOU, *J. Appl. Phys.* **62** (1987) 4821.
9. S. VILMINOT, S. ELHADIGUI, J. P. KAPPLER,

J. C. BERNIER, T. DUPIN, R. BARRAL and G. BOUZAT, *Brit. Ceram. Proc.* **40** (1988) 15.

10. S. VILMINOT, S. ELHADIGUI, A. DERORY, M. DRILLON, J. C. BERNIER, J. P. KAPPLER, R. KUENTZLER and Y. DOSSMANN, *Mater. Res. Bull.* **23** (1988) 521.
11. D. H. A. BLANK, J. FLOKSTRA, G. J. GERRITSMA, L. J. M. van de KLUNDERT and G. S. M. VELDERS, *Physica* **145B** (1987) 222.
12. S. VILMINOT, S. ELHADIGUI and C. HIS, *Physica C* 153–155 (1988) 387.
13. T. H. GEBALLE, M. R. BEAMSLEY, A. KAPITULNIK, R. HAMMOND and J. HARRIS, *Phys. Today* **40(7)** (1987) 19.
14. J. P. SINGH, U. BALACHANDRAN, D. SHI, J. K. DEGENER and R. B. POEPPEL, *Mater. Lett.* **7** (1988) 72.
15. N. E. PHILLIPS, R. A. FISHER, S. E. LACY, C. MARCENAT, J. A. OLSEN, W. K. HAM, A. M. STACY, J. E. GORDON and M. L. TAN, *Physica* **148B** (1987) 360.
16. R. KUENTZLER, Y. DOSSMANN, S. VILMINOT and S. EL HADIGUI, *Solid State Commun.* **65** (1988) 1529.

Received 16 January
and accepted 30 November 1990